HHS Public Access

Author manuscript

Autism Res. Author manuscript; available in PMC 2022 August 01.

Published in final edited form as:

Autism Res. 2021 August ; 14(8): 1554–1571. doi:10.1002/aur.2516.

Differential effects by sex with Kmt5b loss.

Rochelle N. Wickramasekara[1], **Brynn Robertson**[1], **Jason Hulen**[1], **Jodi Hallgren**[1], **Holly A. F. Stessman**[1,*]

[1]Department of Pharmacology & Neuroscience, School of Medicine, Creighton University, Omaha, Nebraska, U.S.A.

Abstract

Lysine methyl transferase 5B (KMT5B) has been recently highlighted as a risk gene in genetic studies of neurodevelopmental disorders (NDDs), specifically, autism spectrum disorder (ASD) and intellectual disability (ID); yet, its role in the brain is not known. The goal of this work was to neurodevelopmentally characterize the effect(s) of KMT5B haploinsufficiency using a mouse model. A *Kmt5b* gene-trap mouse line was obtained from the Knockout Mouse Project. Wild type (WT) and heterozygous (HET) mice were subjected to a comprehensive neurodevelopmental test battery to assess reflexes, motor behavior, learning/memory, social behavior, repetitive movement, and common ASD comorbidities (obsessive compulsion, depression, and anxiety). Given the strong sex bias observed in the ASD patient population, we tested both a male and female cohort of animals and compared differences between genotypes and sexes. HET mice were significantly smaller than WT littermates starting at postnatal day 10 through young adulthood which was correlated with smaller brain size (i.e., microcephaly). This was more severe in males than females. HET male neonates also had delayed eye opening and significantly weaker reflexes than WT littermates. In young adults, significant differences between genotypes relative to anxiety, depression, fear, and extinction learning were observed. Interestingly, several sexually dimorphic differences were noted including increased repetitive grooming behavior in HET females and an increased latency to hot plate response in HET females versus a decreased latency in HET males.

Lay Abstract

Lysine methyl transferase 5B (KMT5B) has been recently highlighted as a risk gene in neurodevelopmental disorders (NDDs), specifically, autism spectrum disorder (ASD) and intellectual disability (ID); yet its role in the brain is not known. Our study indicates that mice lacking one genomic copy of *Kmt5b* show deficits in neonatal reflexes, sociability, repetitive stress-induced grooming, changes in thermal pain sensing, decreased depression and anxiety, increased fear, slower extinction learning, and lower body weight, length, and brain size. Furthermore, several outcomes differed by sex, perhaps mirroring the sex bias in ASD.

Keywords

Mouse models; Genetics; Genotype-Phenotype correlation

*Correspondence: hollystessman@creighton.edu; Tel.: +01-402-280-2255 (H.A.F.S).

Introduction

Several recent high-throughput sequencing studies have implicated lysine methyl transferase 5B (KMT5B) as a risk gene in neurodevelopmental disorders (NDDs), specifically, autism spectrum disorder (ASD) and intellectual disability (ID) (Coe et al., 2019; Faundes et al., 2017; Satterstrom et al., 2020; Stessman et al., 2017; Trinh et al., 2019). This patient population is characterized primarily by *de novo* heterozygous disruptive *KMT5B* variants with comorbidities including global developmental delay, speech/language delay, motor phenotypes, seizures, and structural brain abnormalities (Wickramasekara & Stessman, 2019). Yet, the role this gene plays in the brain is largely unknown.

KMT5B is thought to be the primary enzyme that di-methylates (me2) histone 4 lysine 20 (H4K20) residues. The enzyme is a member of a larger family of SET domain-containing proteins including KMT5A and KMT5C, which establish H4K20 mono- and tri-methylation marks, respectively. Increasing methylation at H4K20 results in chromatin compaction and gene silencing (Kourmouli et al., 2004; Schotta et al., 2004). *Kmt5a* and *Kmt5b* null mouse models have been associated with embryonic or perinatal lethality, while *Kmt5c* null mice have no apparent phenotype (Oda et al., 2009; Schotta et al., 2008), highlighting an importance for KMT5B and H4K20me2 in organismal development. Indeed, H4K20me2 has been implicated in critical cell processes such as, cell cycle, DNA replication, stem cell maintenance, and repair of DNA double-stranded breaks (Boonsanay et al., 2016; Machado & Relaix, 2016; Schotta et al., 2008; Vougiouklakis et al., 2015; Wu et al., 2018).

Rodents have become an attractive model system for studying the pathophysiology of high-risk ASD genes (de Vrij et al., 2008; Gompers et al., 2017; Guy, Hendrich, Holmes, Martin, & Bird, 2001; Zhou et al., 2009). Established neurobehavioral test batteries (Silverman, Yang, Lord, & Crawley, 2010) allow for greater reproducibility and better comparisons across genes to identify both common and divergent pathologies characterizing unique genetic subtypes of ASD/NDD. Furthermore, the work of the Knockout Mouse Project (KOMP) (Austin et al., 2004; Hansen et al., 2008) has made knockout alleles readily-available for most genes in the mouse genome. Such projects give us the ability to quickly screen novel NDD risk genes in mice in a high-throughput way.

Herein, we compare cohorts of *Kmt5b* wild type (WT) and heterozygous (HET) mice using a comprehensive neurodevelopmental rodent test battery. Core domains of ASD—social behavioral deficits and repetitive patterns of behavior—were examined using the three chambered social approach test, social preference test, grooming microstructure analysis, and marble burying test. Additional tests targeted common ASD comorbidities including (1) early developmental milestones (Ferreira and Oliveira 2016), (2) atypical sensory experiences (Balasco, Provenzano, Bozzi 2020; Klintwall et al. 2011), (3) motor deficits (Ming, Brimacombe, Wagner 2007), (4) global intellectual disability and developmental delay (Polyak, Kubina, Girirajan 2015), and (5) anxiety and depression phenotypes (DeFilippis, 2018; Hollocks, Lerh, Magiati, Meiser-Stedman, & Brugha, 2019). Behavioral tests were conducted in young-adult mice to represent adolescent-young adult stages in humans when ASD is often readily apparent (Dutta & Sengupta, 2016). Given the significant sex bias in ASD (Loomes, Hull, & Mandy, 2017), both female and male cohorts were tested.

Methods

Mice

Kmt5b$^{tm1a(KOMP)Wtsi}$ mice on a C57BL/6N background were cryorecovered from the UC Davis Knockout Mouse Project (MGI:2444557, Targeting Project: CSD28648). This gene trapping strategy makes *Kmt5b*$^{tm1a(KOMP)Wtsi\ flox/+}$ mice effectively heterozygous for *Kmt5b*. The genotypes of F2 progeny are expected to be wild type (WT; *Kmt5b*$^{wt/wt}$), heterozygous (HET; *Kmt5b*$^{wt/tm1a}$) or homozygous knockout (KO; *Kmt5b*$^{tm1a/tm1a}$). All mouse work was approved and monitored by the Creighton University Institutional Animal Care and Use Committee (IACUC) under protocol numbers 1039 and 1040. Mice were housed in a temperature-controlled vivarium maintained on a 12-h light–dark cycle with food and water provided *ad libitum*. Mice were weaned at three weeks of age. WT and HET littermates were housed in unisex groups of 2–5 mice of the same litter in individually ventilated cages. Behavioral experiments and sample collection were performed during the first five hours of the light phase. Mouse genotypes were determined from tail biopsies using real time PCR with specific probes designed for the WT *Kmt5b* and LacZ sequences (Transnetyx, Cordova, TN).

HET x HET mating was used to determine Mendelian genotypic ratios at E14.5, ~E17.5, P0 and > P21. WT x HET mating was used to generate animals for behavioral experiments. All adult behavioral testing was performed in a temperature-, sound-, and light-controlled mouse behavioral room at Creighton University. All mice were housed in this behavior room for at least 48 hours prior to experimenting; thus, mice were well-acclimated to the testing environment. All tests (unless otherwise noted) were video recorded and scored retrospectively by investigators who were blind to the genotype.

qRT-PCR

Kmt5b transcript levels were detected using qRT-PCR on E14.5 embryonic brain tissue dissected from HET X HET time mated dams. RNA was extracted using the RNeasy Mini Kit (Qiagen, Hilden, Germany) including DNase I treatment (Qiagen) to eliminate genomic DNA and quantified using the Qubit 3.0 Fluorometer and RNA BR Assay Kit (Invitrogen; Waltham, MA). cDNA libraries were generated using iScriptTM Reverse Transcription Supermix (Bio-Rad; Hercules, CA). qPCR was performed using SsoAdvanced Universal SYBR Green Supermix (Bio-Rad; Hercules, CA) on a CFX Connect instrument (Bio-Rad) using PrimeTime® qPCR Primers (Integrated DNA Technologies; Coralville, IA) for *Kmt5b*/*Suv420h1* (Mm.PT.58.9787344 [exon 7–8] and Mm.PT.58.14076858.g [exon 1–2]). All data were normalized to proprietary PrimePCR™ PCR (Bio-Rad) primer set: GAPDH (qMmuCED0027497) expression.

Histone Protein detection

H4K20me1, me2, and me3 levels were detected in E14.5 embryonic brain tissue from HET x HET offspring using western blotting. Histone protein extraction was performed using a Histone Extraction Kit (Abcam; Cambridge, United Kingdom) according to the manufacturer's instructions. Protein extracts were separated on a Mini Trans-Blot Cell (Bio-Rad; Hercules, CA) system using 4–20% Mini-PROTEAN TGX Gels (Bio-Rad; Hercules,

CA), transferred using the Trans-Blot® Turbo™ Transfer System (Bio-Rad; Hercules, CA) using pre-assembled Trans-Blot Turbo Mini 0.2 μm PVDF Transfer Packs (Bio-Rad; Hercules, CA), and blocked with EveryBlot Blocking Buffer (Bio-Rad; Hercules, CA). Protein membranes were incubated with rabbit polyclonal anti-H4K20me2 (ab9052) and anti-H4 (ab10158) primary antibodies (Abcam; Cambridge, United Kingdom), washed in TBS buffer (Thermo Scientific; Waltham, MA) with 0.1% Tween-20 followed by a Goat Anti-Rabbit IgG H&L (HRP) (ab205718) secondary antibody (Abcam; Cambridge, United Kingdom). The blots were developed using Clarity™ Western ECL Substrate (Bio-Rad; Hercules, CA). The Precision Plus Protein™ WesternC™ Standard (Bio-Rad; Hercules, CA) was used as a molecular weight marker. Membranes were visualized using a ChemiDoc™ XRS+ System (Bio-Rad; Hercules, CA).

Behavioral Experiments

Three independent cohorts of mice were used to generate behavioral data. This strategy was chosen to increase the number of tests that could be performed while decreasing overall animal usage. The order of testing within each cohort was selected based on least stressful to more stressful test, and stressful tests were distributed across the cohorts. A detailed timeline of assays performed on each cohort are listed in Table S1. Cohort 1 animals were used to test developmental milestones and for the following tests in this order: surface righting, grip strength, open field, social approach, social preference, marble burying, buried fold olfactory, balance beam, rotarod, hot plate. Cohort 2 animals underwent the following tests in this order: olfactory habituation/dishabituation, elevated plus-maze, light↔dark, fear conditioning/recall/extinction. Cohort 3 animals underwent the following tests in this order: grooming microstructure, Barnes maze, foot shock, forced swim.

Neonatal development

Reflex testing (palmar grasp reflex and surface righting) began on PND10 (the earliest age young mice could be ear tagged reliably). We refrained from using paw tattoos that could affect motor behavior testing. Additional neonatal tests—grip strength (PND11), front limb suspension (PND11) and hind limb suspension (PND12)—were performed as previously described (Feather-Schussler & Ferguson, 2016) within a microisolator hood in the Creighton University Animal Resource Facility. Experimental animals in this cohort (Table S1) were also scored for age at incisor eruption (PND10; yes/no), eye opening, pinna folding, and vaginal opening (females only).

Social and repetitive behaviors testing

Pro-social behaviors were scored using a three-chambered sociability box for a two-part social approach-social preference test as described previously (Yang, Silverman, & Crawley, 2011). ANY-maze software was used to track the amount of time the animal's head (body point tracking) spent within a defined 2 cm diameter of each enclosure/total test time, the amount of time spent in each chamber, and the number of transitions between chambers.

Repetitive behaviors were scored using the marble burying test (Chang, Cole, & Costa, 2017) and grooming tests as previously described (Kalueff, Aldridge, LaPorte, Murphy, & Tuohimaa, 2007). For the marble burying test, standard hamster cages with taller walls were

filled with 2.5 cm of mouse bedding. Opaque dividers were used between cages. Mice were allowed to habituate to the bedding for five minutes, after which twelve equal sized marbles were arranged in 4 × 3 equidistant rows. Mice were allowed a total of 30 minutes to explore and dig. At the end of the test, an experimenter live scored the marbles that were buried (>50% marble covered by bedding material). Grooming behaviors were assessed using a two-part test. First, novelty-induced grooming was examined by placing mice in a transparent cylindrical plexiglass enclosure on a smooth surface for 10 minutes. A mirror was placed behind the enclosure for better visualization of video recorded grooming behaviors. Secondly, stress-induced grooming was induced in the same enclosure by misting the animal with sterile water and recording as before for five minutes. Grooming sequences were scored manually as previously described: 1 – elliptical strokes, 2 – unilateral strokes, 3 – bilateral strokes and 4 – body licking (Kalueff et al., 2007).

Sensory tests

Sensory tests included hot plate (Philip et al., 2010), buried food (Yang & Crawley, 2009) and olfactory habituation-dishabituation (Arbuckle, Smith, Gomez, & Lugo, 2015). Thermal nociception at 52° C was assessed using a hot plate (IITC Life Science, Series 8, model 39) with temperature verification using an infrared temperature gun (Etekcity Infrared Thermometer). The latency to show a nociceptive response with hind paw lick, hind paw flick, vocalization, or a jump was recorded. To test olfaction, 24-hour food deprived mice were timed on their ability to identify a buried food treat. For the olfactory habituation-dishabituation test, non-social and social odor preferences were also assessed using three repeated presentations of water, banana, and almond scents followed by scents from two different “stranger” mouse cages, as previously described (Arbuckle et al., 2015).

Exploration, anxiety, depression, and fear tests

Exploration, anxiety, depression, and fear were scored using an open field (Seibenhener & Wooten, 2015), elevated plus maze (Walf & Frye, 2007), light↔dark box (Takao & Miyakawa, 2006), forced swim (Can et al., 2012), and foot shock (Yadav et al., 2013) tests as previously described. For the open field, light↔dark, and elevated plus-maze tests, mice were allowed to explore each of these arenas for ten, five, and ten minutes, respectively, prior to the start of testing. Digital scoring was performed using video recordings and ANY-maze behavior tracking software with body point tracking (Stoelting Co, Wood Dale, IL). The forced swim test was performed over four minutes; total immobile (floating) and mobile (swimming/climbing) time were scored. Freezing behavior to increasing intensity foot shocks was assessed in the same fear conditioning apparatus described below. Following a two-minute acclimation period, a series of foot-shocks (two seconds each) were delivered ranging from 0.1 to 0.8 mA at 0.1 mA ascending increments with a 30 sec ITI. Freezing behavior was scored using the automated ANY-maze freezing software.

Learning and memory tests

Fear conditioning, recall, and extinction were performed in a sound-attenuating isolation cabinet: ugo basile ANY-maze controlled fear conditioning system (Stoelting Co, Wood Dale, IL). On fear acquisition day one, the mouse was placed in a 17 × 17 × 25(h) cm chamber fitted with a metal grid floor fitted inside the sound-attenuating cabinet. Following

a 120s habituation period, the mouse was presented with three pairings of a conditioned stimulus (CS, 30 seconds in duration, 2000 Hz tone) which co-terminated with an unconditioned stimulus (US, 2 seconds in duration, 0.8 mA scrambled foot shocks). The inter-trial intervals between each pairing was 90, 60 and 30 seconds respectively. Following a 120 second no-stimulus consolidation period, the mouse was returned to a clean holding cage to avoid fear transfer to non-tested mice. All animals were later returned to their home cage once testing was complete. Freezing behavior (recorded as absence of all non-respiratory movements) was scored using automated ANY-maze software. Fear acquisition was examined using freezing scores for the 30 seconds after each CS-US pairing. On day two, contextual fear recall was examined by introducing the mouse back into the chamber fitted with a metal grid floor. While the 80 dB white noise was played for the duration of the session, there was no CS or US presentation. Freezing behavior was monitored for ten minutes, after which the mouse was placed in a clean holding cage until all testing was complete. Freezing scores for context fear recall are presented as the SEM of the mean for the entire duration of the test. On day three, mice were transferred to a new holding area surrounded with checkerboard patterned walls and transferred to a new cage containing lemon essence to change the environment. The chamber previously fitted with a metal grid floor was now covered with smooth flooring, the chamber walls were changed to black and white patterned prints and mild lemon essence were used to present new visual, tactile and odor cues. After a 120 second habituation period, the mouse was presented with 40 CS presentations (2000 Hz tone) with an inter-trial-interval (ITI) of 10s. The freezing response was recorded as before and is expressed in blocks of two stimuli.

The Barnes maze test was performed as previously described (Rosenfeld & Ferguson, 2014) using a 12 day protocol to assess spatial learning. The maze (Stoelting Co) was enclosed by carboard walls and visual cues were placed around the maze. On days one through eight (learning phase), mice were allowed to explore the maze and find the escape hole within two minutes. Mice who failed to enter the escape were guided to the target and allowed to remain for 30 seconds. The location of the escape hole remained the same during the learning phase. On day nine, a probe trial was conducted with the escape hole in the same location. Reversal learning was conducted on days 10–12 where the escape hole was rotated by 180°. Two trials were conducted each day during all phases. The time to enter the escape hole, distance to escape hole, primary latency and search strategies (Pitts, 2018) were recorded.

Motor behavior tests

Motor behavior and coordination were assessed using an elevated balance beam (Luong, Carlisle, Southwell, & Patterson, 2011) and rotarod (Deacon, 2013). For the balance beam test, mice were scored based on the total time to cross beams of two different widths (12 and 6 mm). For the rotarod test, a four-lane rotarod (Rotamex 5, Columbus Instruments, Columbus, OH) was used and accelerated from 4–40 rotations per minute (RPM) over five minutes total until the animal could no longer maintain its position on the rod; at this point, both the RPM and the total time were recorded.

Brain histology

Animals were deeply anesthetized and transcardially perfused with 1X phosphate-buffered saline (PBS) followed by 4% paraformaldehyde in 1X PBS. Brains were removed from the skull and postfixed in 4% paraformaldehyde. Brains were cryoprotected in 30% sucrose, embedded in optimal cutting temperature compound (VWR; Radnor, PA) and frozen in preparation for cryosectioning. Coronal 40-μm thick sections were made using a cryostat (Leica Biosystems; Wetzlar, Germany). Sections were Nissl-stained with 0.1% cresyl violet (Abcam; Cambridge, United Kingdom) to identify brain structures. Sections were dehydrated, cleared in histoclear, and coverslipped using cytoseal mounting media (VWR; Radnor, PA). They were imaged using a VS120 Virtual Slide Scanner (Olympus; Tokyo, Japan) using the 10X objective. ImageJ software was used for measurements (National Institutes of Health, Bethesda, MD, USA) by an observer blinded to genotype. For analysis of the width of several brain regions, the length of d1–d5 was measured at bregma, + 0.86 to +1.18 mm according previously published methods (Mizoguchi et al., 2017). The width of each brain region was defined as follows: d1=whole brain, d2-d3=striatum, d5=motor cortex, d1-d2=somatosensory cortex, d4=septum. The mouse brain in stereotaxic coordinates atlas (Franklin & Paxinos, 2008) was used to locate each brain region.

Data analysis

Quantitative RT-PCR and western blotting data were analyzed using either a Welch's or Brown-Forsythe ANOVA test followed by a Dunnett's T3 multiple comparisons post hoc test. Motor reflex tests were analyzed for differences between genotypes (WT and HET) using a 2-way ANOVA (with independent variables genotype and litter). All behavioral tests were analyzed for differences between genotypes (WT and HET) and sexes using a 2-way ANOVA. Post hoc tests (Tukey's or Sidak's multiple comparisons tests) were used to identify specific differences. In the case of repeated measures (e.g., fear conditioning), a 3-way ANOVA or mixed-effects model (REML) were used followed by Tukey's multiple comparisons or Fisher's LSD test (post hoc). A p-value < 0.05 was considered significant in all tests. A minimum of nine animals per genotype and sex were used for all experiments based on similar previous studies (Crawley, 2007). Animals that did not initiate the test were eliminated from analysis. All analyses were performed using GraphPad Prism v8. All graphs show the mean ± SEM.

Results

Kmt5b loss effects manifest early in postnatal life.

To characterize neurobehavioral deficits resulting from KMT5B loss, we obtained a cryorecovered mouse line harboring a 'knockout-first' allele at the *Kmt5b* locus. Insertion of the gene trap cassette between *Kmt5b* exons 4 and 5 results in splicing from exon 4 to the En2 SA (splice acceptor) site in the cassette which drives the expression of the lacZ/neo selectable marker immediately terminated by a pA (polyadenylation signal) (Figure S1). This construct effectively creates an early truncation upstream of the *Kmt5b* functional SET domain. Mice that are wild type, heterozygous and homozygous null for the gene trap allele were referred to as WT, HET and KO, respectively. In order to validate the gene trap, quantitative RT-PCR was performed using embryonic day (E) 14.5 whole brain cDNA which

showed significant downregulation of *Kmt5b* transcripts (Exon 7–8) in HET and KO compared to WT ($W_{(2, 7.842)}$=8.619; p=0.0104; Welch's ANOVA; Figure 1A). Although the known function of KMT5B is di-methylation of H4K20 residues (Schotta et al., 2004; Schotta et al., 2008), H4K20me2 and H4K20me3 protein levels were not significantly different across genotypes (Figure 1B–C) by western blot. This is likely related to the secondary function of H4K20me2 in detection and resolution of DNA double-stranded breaks (Jorgensen, Schotta, & Sorensen, 2013; Paquin & Howlett, 2018), known dynamic changes of H4K20me2 and me3 related to cell cycle (Pellegrino, Michelena, Teloni, Imhof, & Altmeyer, 2017; Simonetta et al., 2018), and/or a lack of regional specificity with using whole brain homogenates. H4K20me1 levels, however, were significantly increased in HET and KO embryonic brain tissue compared to WT ($F^*_{(2, 4.711)}$=16.33; p=0.0076; Brown-Forsythe ANOVA; Figure 1D), which has been reported previously in mouse embryonic fibroblasts collected from a *Kmt5b*/*Kmt5c* double knockout mice (Schotta et al., 2008).

HET x HET progeny collected over a developmental time course showed significantly reduced Mendelian ratios for the KO genotype starting at postnatal day (P) 0 (Table 1) suggesting late-term or perinatal lethality. Indeed, an independently-derived model has also shown that *Kmt5b*-null pups that are born die shortly after birth (Schotta et al., 2008). Intercrosses of HET mice were often non-productive and produced fewer viable offspring than HET x WT mating (data not shown). Because dams often cannibalized dead pups, necropsy to determine the cause of death was not possible. Interestingly, KO embryos were present at expected Mendelian ratios as late as E18.5 without any obvious gross developmental abnormalities (not shown). WT and HET progeny from WT x HET mating were subjected to a comprehensive neurodevelopmental test battery to identify behaviors that may be consistent with the *KMT5B* patient population. Given the strong sex bias observed in the ASD patient population (Loomes et al., 2017), we tested both male and female cohorts of animals and compared differences between genotypes and sexes.

Testing on pre-weaned pups focused on developmental milestones, reflexes, coordinated movement, and equilibrium. Importantly, surface righting, grip strength, front and hindlimb suspension tests were tested prior to the onset of fear (postnatal day; P10–12) (Hartley & Lee, 2015; Landers & Sullivan, 2012). Palmar grasp reflex was either fully or weakly present in all animals at PND10 with no significant differences between groups (Fisher's exact test; Figure 2A). Observation of additional developmental milestones in these mice showed no differences in incisor eruption (not shown), pinna folding (Figure 2B), or vaginal opening in females (Figure 2C). However, eye opening was significantly impacted by genotype ($F_{(1, 44)}$=7.619; p=0.0084; 2-way ANOVA; Figure 2D). Post hoc analysis showed that this effect was driven primarily by males (Sidak's multiple comparisons p=0.0408). The surface righting reflex was also present in all animals at PND10; however, the time to right varied significantly by litter (not shown). Body weight is known to be inversely correlated with litter size in mice (Epstein, 1978). A simple linear regression analysis between body weight and time to right showed a significant correlation among HET females (Figure S2). However, poor performance in neonatal testing could also be due to maternal care (Brunelli et al., 2015; Curley & Champagne, 2016; Ellenbroek, Derks, & Park, 2005), which we could not independently control for in this test. Therefore, neonatal data (surface righting, grip strength, front and hindlimb suspension) were corrected for litter and are presented as litter

averages between genotypes for each sex separately. After litter correction, male HET but not female HET mice are significantly slower to right in this test from a supine position ($F_{(1, 25)}$=12.31; p=0.0017; 2-way ANOVA; Figure 3A–B). A similar trend was seen in the grip strength test ($F_{(1, 28)}$=4.318; p=0.0470; 2-way ANOVA; Figure 3C–D) where male HET animals fell sooner (i.e., at a lower angle) than their male WT littermates. In both the front limb ($F_{(1, 19)}$=10.14; P=0.0049; 2-way ANOVA; Figure 3E–F) and hindlimb ($F_{(1, 20)}$=6.610; p=0.0182; 2-way ANOVA; Figure 3G–H) suspension tests, male HET animals were less capable of resisting the force of gravity on their bodies (reported as “hanging impulse (time to fall (s)/weight (g))”) than their male WT littermates.

Young adult Kmt5b HET mice show differences in social preference, grooming, anxiety, depression, and fearfulness.

To assess core ASD behaviors, we used a two-part social approach and social preference test, a marble burying test, and scored grooming microstructures. Analysis of the social approach data revealed a lack of sociability for all animal groups in this test (Figure 4A) suggesting no meaningful comparisons could be drawn. When given the preference between a familiar or novel mouse (social preference), WT females, but not WT males, met the sociability criteria (i.e., a significant preference for the novel versus familiar mouse; Fisher’s LSD p=0.0057; Figure 4B). A 2-way ANOVA among females between genotype and interacting partner (familiar versus novel mouse) showed a significant main effect of interacting partner ($F_{(1, 44)}$=4.461; p=0.0404); post hoc testing revealed no social preference in HET females (Sidak’s multiple comparisons p=0.7608; Figure 4B).

Marble burying and self-grooming were used to assess repetitive behavior. There were no significant differences between sexes or genotypes in the marble burying test (Figure 4C). Rodent grooming is known to follow a structured sequence that consists of repeated stereotyped movements (Kalueff et al., 2016). We quantified self-grooming, as previously described, by scoring the four phases of the cephalo-caudal grooming pattern (phase 1 = nose; phase 2 = face; phase 3 = head; phase 4 = body) (Kalueff et al., 2007) under both a novelty-induced (novel environment) and stress-induced (misted with water) condition. Stress stimulus resulted in significantly more grooming ($F_{(1, 96)}$=93.78; p<0.0001; 3-way ANOVA) compared to a novel environment. Post hoc testing showed that this effect was similar across all sexes and genotypes (Figure 4D). Considered separately, there was a significant interaction between genotype and sex in the percent of time spent grooming in the stress-induced ($F_{(1, 48)}$=6.668; P=0.0129; 2-way ANOVA; not shown), but not the novelty-induced grooming test. However, no individual comparison survived post hoc testing.

For each phase of grooming, the number of initiations, percent of time spent, and sequence (i.e., phase order) were compared. The percent of time devoted to each phase of grooming was different following novel- and stress-stimulus (Figure S3A–B). However, independent analyses of novelty-induced and stress-induced grooming patterns between sexes and genotypes showed no significant differences in the distribution of grooming time across phases by stimulus (Figure S3A–B). Three-way ANOVA analysis of the number of phase initiations suggested a significant interaction between sex and genotype during stress-

induced grooming ($F_{(1, 192)}$=4.202; p=0.0417; Figure 4E). Post hoc testing showed this effect was driven by an increased number of phase three (head grooming) initiations in HET females compared to WT females after stress stimulus (Tukey's multiple comparisons p=0.0042; Figure 4E) but no differences during novelty-induced grooming (Figure S3C). The rate of phase transitions did not significantly differ between sexes or genotypes (not shown). While the overall transition error rate significantly decreased after stress stimulus ($F_{(1, 97)}$=10.26; p=0.0018; 3-way ANOVA), no individual comparison survived post hoc testing (Figure S3D). Analysis of correct phase transitions suggested that this was likely due to a genotype x sex x sequence interaction ($F_{(5, 288)}$=6.242; p<0.0001) driven primarily by a repeated phase 3–4 pattern that was significantly increased in HET compared to WT females (Tukey's multiple comparisons p<0.0001; Figure 4F).

Sensory issues were tested using hot plate, buried food olfaction, and olfactory habituation/dishabituation tests. For the hot plate test, there was a significant interaction between sex and genotype ($F_{(1, 35)}$=10.27; 2-way ANOVA; p=0.0029; Figure 5A); however, there was a clear difference in response by sex. Post hoc analysis using a Fisher's LSD test showed that male HETs had a significant decrease in latency (p=0.0249) whereas female HETs showed an increase in latency (p=0.0347) to a 52° C thermal nociceptive stimulus (Figure 5A). Overall, WT females showed a lower yet non-significant latency (i.e., increased sensitivity) to thermal pain compared to WT males (Fisher's LSD p=0.0528), which is consistent with both the rodent and human literature (Hurley & Adams, 2008). In the buried food olfaction test, genotype had a moderate yet non-significant effect ($F_{(1, 38)}$=3.948; p=0.0542; 2-way ANOVA; Figure 5B). Sequential presentation of both non-social and social odors using the olfactory habituation/dishabituation test show that all groups have a greater response to social versus non-social odors (Figure 5C–D). However, no significant differences in odor habituation/dishabituation were identified between genotypes or sexes (Figure 5C–D).

Kmt5B mice show differences in anxiety, depression, and fear related to sex and genotype.

An open field, elevated plus-maze, light↔dark box, forced swim, and foot shock tests were used to score exploration, anxiety, depression, and fearfulness. No significant differences were observed for the mean speed and distance traveled (not shown), nor the number of center entries (Figure 6A) or percent of time spent in the center of the open field (Figure 6B) between genotypes or sexes. While total arm entries in the elevated plus-maze did not differ between groups (Figure 6C), females showed significantly more open arm entries in this test than males ($F_{(1, 44)}$=4.176; p=0.0470; 2-way ANOVA; Figure 6D). A three-way comparison between sex, genotype, and the percent of time spent in each arm type (closed versus open) confirmed that all groups had a significant preference for the closed arms ($F_{(1, 88)}$=1318; p<0.0001; 3-way ANOVA;) that survived post hoc testing (Tukey's multiple comparisons p<0.0001 for all groups); yet, there were no significant differences between sexes or genotypes (Figure 6E). In the light↔dark box test, we identified a significant increase in total light↔dark transitions in female mice independent of genotype ($F_{(1, 45)}$=11.20; p=0.0017; 2-way ANOVA; Figure 6F). A comparison of sex and genotype on the percent of time spent in each box (dark versus light) showed no significant main effect of sex or genotype, but post hoc testing did show that both male and female WT animals had a

significant preference for the dark box (as expected; Figure 6G). While this same trend was observed among HET animals, the degree of this preference was reduced (Figure 6G).

For the forced swim test, we calculated the percent of time spent immobile (floating) versus mobile (swimming/climbing) and compared these against sex and genotype. Male and female WT mice performed similarly in this test with greater immobile compared to mobile time (Tukey's multiple comparisons $p<0.0001$ for both; Figure 6H). There was no main effect of sex in this test; however, here was a significant interaction between genotype and mobile/immobile time ($F_{(1, 96)}=6.241$; $p=0.0142$; 3-way ANOVA; Figure 6H). This effect appears to be driven primarily by males as the male HET genotype showed no significant difference between mobile and immobile time in this test. In the foot shock threshold test, we identified a significant difference in freezing time for both sex ($F_{(1, 363)}=11.46$; $p=0.0008$; 3-way ANOVA) and genotype ($F_{(1, 363)}=15.92$; $p<0.0001$; 3-way ANOVA) yet no significant interactions. HETs had increased freezing time following foot shock in both sexes; this effect was stronger in females (Figure 6I–J) suggesting increased fearfulness among HETs. No individual comparisons survived post hoc testing.

Comorbid behavioral tests suggest differences in extinction learning but not motor behavior.

Common ASD comorbidities that have been observed among many *KMT5B* patients are intellectual disability and motor deficits. Learning and memory were scored in this mouse model using fear conditioning and the Barnes maze. In our fear conditioning paradigm, the fear acquisition phase showed that a paired conditioned stimulus (2000 Hz tone) and unconditioned stimulus (0.8 mA foot shock) stimulated fear (measured as significantly increased freezing behavior ($F_{(3, 100)}=54.76$; $p<0.0001$; 3-way ANOVA) similarly across both sexes and genotypes (Figure 7A). Context recall in the absence of stimulus was tested the following day. Sex contributed significantly to recall ($F_{(1, 45)}=12.95$; $p=0.0008$; 2-way ANOVA; Figure 7B) where females had less recall independent of genotype. Cue recall and extinction were tested on day three in a novel environment. All animals did present fear renewal to the conditioned stimulus in the novel environment; however, this was only significant among males (Figure 7C; $p\leq0.0016$; Fisher's LSD). Significant main effects of sex ($F_{(1, 900)}=161.5$; $p<0.0001$; 3-way ANOVA) and genotype ($F_{(1, 900)}=7.658$; $p=0.0058$; 3-way ANOVA) were identified, but no significant interactions between any of the test variables. As during context recall, females showed significantly lower freezing times during cue recall than males independent of genotype ($F_{(1, 940)}=170.5$; $p<0.0001$; 2-way ANOVA; Figure 7C). Analysis of genotype independent of sex showed a significant difference between HET and WT animals ($F_{(1, 940)}= 14.64$; $p=0.0001$; 2-way ANOVA) during cue recall/extinction. Fisher LSD post hoc testing could not identify where female WT and HET samples diverged in this test; however, in males, this appears to be around the time of extinction in WTs (Figure 7C), suggesting that extinction learning may be affected in HET males.

The Barnes maze was used to score hippocampal-dependent learning. Acquisition was performed over eight days, followed by a test/probe day, and three additional days of reversal (i.e., moving of the escape box). Time to find the escape hole (Figure S4A–B) and

total distance to find the escape hole (Figure S4C–D) were scored. Overall, performance in this test was significantly affected by sex ($F_{(1, 504)}$=76.82; p<0.0001; 3-way ANOVA) where females found the escape hole more quickly; therefore, the sexes were analyzed separately. Visual analysis of these data suggested that our mouse line does not perform in this test as expected (i.e., no significantly increased times upon reversal in WT animals). Interestingly, when we analyzed the search patterns (random, serial, or spatial) (Pitts, 2018) utilized on training (Figure S4E) and test day (Figure S4F) in our animals, we saw a significant transition from random to non-random (serial or spatial) searching for both WT and HET animals (WT-M p=0.0373; HET-M p=0.0002; WT-F p=0.0013; HET-F p=0.0112; Fisher's exact tests). There were no significant differences between searching patterns at any timepoint between sexes or genotypes, and the expected spatial (cue-based) searching strategy was not the predominate strategy used in any group except female HETs. A lack of expected performance in WT animals in this test made these data difficult to interpret.

Motor behavior was scored using elevated balance beam and rotarod tests. Two widths of balance beam were used, 12 mm (Figure 8A) and 6 mm (Figure 8B). There were no significant interactions between sex and/or genotype in this test. There was, however, a significant main effect of sex in the 6 mm test ($F_{(1, 35)}$=7.651; p=0.0090, 2-way ANOVA; Figure 8B). For the rotarod test, there was a modest yet significant difference between sexes, but not genotypes, for the average time to fall ($F_{(1,42)}$=4.478; p=0.0403; 2-way ANOVA; Figure 8C). Females generally outperformed males in this test, which is consistent with other studies (Tucker, Fu, & McCabe, 2016). The rotarod test also carries a learning component where wild type mice will remain on the rod longer with each successive trial until fatigued (Buitrago, Schulz, Dichgans, & Luft, 2004). We find this trend among our WT females but not WT males (not shown). A comparison of the time to fall between trial three compared to trial one on the rotarod was not statistically different between sexes or genotypes (Figure 8D) suggesting no differences in learning in this test.

Kmt5b contributes substantially to body weight, length, and brain size.

Given the motor deficits observed in our behavioral testing battery, we assessed body weight over the behavioral testing window (P10-P44). WT weights diverged between sexes after weaning but before P35, consistent with the onset of puberty (Brust, Schindler, & Lewejohann, 2015) (Figure S5A). Analysis of the effect of age, sex, and genotype on weight show a significant interaction ($F_{(9, 442)}$=2.174; p=0.0228; REML). Independent analyses of age and genotype on weight by sex show that both male and female HET mice have significantly reduced body weight compared to their WT counterparts (Figure 9A–B). This was more significant in males ($F_{(1, 43)}$=42.86; p<0.0001; REML; Figure 9A) than females ($F_{(1, 52)}$=17.60; p=0.0001; REML; Figure 9B). Further, P44 HETs showed a significant interaction between sex and genotype in body length (tail excluded) ($F_{(1, 54)}$=5.548; p=0.0222; 2-way ANOVA; Figure 9C). Females, overall, were significantly shorter than males ($F_{(1, 54)}$=51.12; p<0.0001; 2-way ANOVA), which was expected at this age (Bergmann, Militzer, Schmidt, & Buttner, 1995). Although HET mice were significantly shorter than WT regardless of sex ($F_{(1, 54)}$=35.69; p<0.0001; 2-way ANOVA), this was driven primarily by the male HETs (Tukey's multiple comparisons p<0.0001; Figure 9C). This pattern was consistent with mouse body weights (Figure 9A–B).

Given the consistently smaller body sizes and weights among HET mice and known cases of microcephaly in the ASD population (Fombonne, Roge, Claverie, Courty, & Fremolle, 1999), we took measurements (Figure S5C–E) from adult mouse brains that were dissected following behavioral testing. Three-way ANOVA testing between sex, genotype, and brain region showed a significant interaction between region and genotype ($F_{(4, 110)}$=5.620; p=0.0004). Post hoc testing showed that this effect was likely driven by smaller whole brain size in HET males (Figure 8D–E).

Discussion

Our NDD-focused test battery revealed significant differences in the KOMP *Kmt5b* gene trap HET mouse model in neonatal development, social preference, repetitive stress-induced grooming, depression, anxiety, fear, thermal nociception, extinction learning, body weight and length, brain size, and viability. With the exception of embryonic/perinatal lethality in *Kmt5a*$^{-/-}$ (Oda et al., 2009) and *Kmt5b*$^{-/-}$*Kmt5c*$^{-/-}$ (Schotta et al., 2008) animals, we are not aware of any other studies that have been published regarding how the KMT5 gene family affects behavior or neurodevelopment. The modest effect size of many of the changes we have observed is highly reminiscent of other mouse models of ASD-risk genes that have been published, such as *CHD8*, another chromatin modifying ASD candidate gene (Gompers et al., 2017). Interestingly, many of the significant behavioral effects observed required stress for presentation (e.g., stress-induced grooming and conditioned stimulus). Perhaps these effects are not surprising given the often-subtle phenotypes of ASD patients, which has historically made detection and diagnosis difficult. These data do, however, give us some insights into which structures in the brain might be most affected in our model. For example, it is known that extinction learning involves the medial prefrontal cortex (mPFC) which projects to inhibitory cells located in the amygdala (Schiller & Delgado, 2010). These cells integrate information from the basolateral amygdala (bLA) and mPFC to inhibit central amygdala nucleus (CE) output, thus facilitating extinction consolidation (Schiller & Delgado, 2010). However, the bLA is also strongly implicated in fear acquisition in conditioned-unconditioned fear stimulus paradigms (Singewald & Holmes, 2019). Given that fear acquisition is no different between WT and HET animals (Figure 6A), we believe the mPFC to be the most interesting target for future study.

Several sexually dimorphic phenotypes were observed in this mouse model. Females, regardless of genotype, had more transitions in the light↔dark test and more light arm entries in the elevated plus-maze, suggesting greater risk-taking or novelty-seeking behavior (Bailey & Crawley, 2009). Females were also able to maintain posture on the rotarod longer than males. Interestingly, such behaviors (novelty-seeking and motor behavior/endurance) are known to change in WT mice over time (Shoji, Takao, Hattori, & Miyakawa, 2016). The dimension of time (i.e., aging) was not considered in this study; however, this should be a focus of future work to better understand how ASD and comorbid symptoms may improve or worsen over time. Context recall in our fear conditioning paradigm was lower in females than males suggesting reduced memory consolidation (Myers & Davis, 2007). Finally, female HETs displayed less sensitivity to heat, whereas male HETs had increased sensitivity to heat. Perhaps most interesting, males in this study were more severely affected during early development and in body and brain size over the testing period whereas females were

most affected in ASD-relevant tests (social preference and repetitive grooming). For males, these effects started early (P10–12) with delayed milestones, slower reflexes, and low body weight. While female HETs caught up to their WT littermates in body weight around the start of puberty (P35), this did not happen in males, suggesting perhaps a female protective effect surrounding body weight. This effect may give females HETs an advantage to reproduce over male HETs. A clear limitation to these observations is that male WT animals did not perform as expected in the social preference test. Most certainly female estrous cycles (which we did not control for) also contributed to some tests in our battery increasing inter individual variability and reducing our power (such as in the social approach and social preference tests). Nonetheless, the differences between sexes in this model should be investigated further.

A consistent finding across sexes was low body weight, length, and brain size in HET animals compared to WTs; this effect was larger in males than females. A portion of *KMT5B* human patients have also been reported with growth problems (Wickramasekara & Stessman, 2019). Given the links between H4K20 methylation and cell proliferation (Vougiouklakis et al., 2015; Wu et al., 2018), it is tempting to hypothesize that this effect is due to changes in cell proliferation. Lean muscle mass and body fat are known to contribute substantially to body weight in mice (Reed, Bachmanov, & Tordoff, 2007). Published work suggests that KMT5B is required for the maintenance of adult muscle stem cell progenitor pools which are required for regenerating muscle fibers (Boonsanay et al., 2016; Machado & Relaix, 2016; Neguembor et al., 2013). It is possible that proper embryonic/neonatal muscle development requires two wild type *Kmt5b* alleles as well. Indeed, our earliest reflex tests suggest male HET neonatal mice have low muscle tone. Muscle hypotonia would most certainly also make individuals less successful when competing for resources which could further compound body weight measurements. Other sensory changes could also contribute to resource acquisition but results of our other behavioral tests argue against major deficits in hearing, vision, and smell. Future experiments will be needed to determine the role of KMT5B in developing muscle.

It is possible that HET pups received poorer maternal care prior to weaning resulting in persistent growth retardation and/or changes in adult behaviors such as exploration/novelty-seeking, grooming, and sociability (Brunelli et al., 2015; Curley & Champagne, 2016; Curley, Davidson, Bateson, & Champagne, 2009; Ellenbroek et al., 2005). Indeed, we did find that litter was a significant variable in our neonatal tests that could not be fully explained by weight (Figure S2). This indicates that some phenotypes may have been compounded by the genotype of the dam, as experimental animals were produced by both WT and HET mothers. We did not originally power our study to test the genotype of the mother as a variable, but we have plotted several tests presented in this study relative to the genotype of the dam (Figure S6). While we did not identify any significant interactions between performance and genotype of the dam in these tests, future work should test this variable directly by both using only WT dams and/or fostering HET progeny onto WT littermate dams. One clear caveat in this study was a lack of social communication testing (i.e., ultra-sonic vocalizations) which is often used to assess ASD-relevant interactions including those between pup and dam (Brunelli et al., 2015; Chang, Cole, & Costa, 2017).

Consortium initiatives have made knock-out alleles for most genes available through the Knockout Mouse Project (KOMP); however, these have largely been constructed on a C57BL/6N background (Hansen et al., 2008). While this allows for relatively high throughput testing of high-risk NDD genes, this strain background may not be ideal for identifying robust neurobehavioral phenotypes. A comprehensive comparison of C57BL/6 substrains showed that C57BL/6N animals have less overall locomotor activity, explore less, and are more anxious than C56BL/6J animals (Matsuo et al., 2010). Indeed, we found that our C57BL/6N WT animals did not perform in many tests (social approach, males in social preference, Barnes maze, and novel object recognition (not shown)) with the dynamic range expected from a C56BL/6J strain, which made the detection of subtle changes between WT and HET difficult. Of the tests commonly assessed in ASD patients, the only one where C57BL/6N mice may be favored is in pre-pulse inhibition (PPI) (Matsuo et al., 2010), a test of sensorimotor gating (Madsen, Bilenberg, Cantio, & Oranje, 2014) and a potential biomarker of schizophrenia (Mena et al., 2016) that was not tested here. While an argument could be made that strain differences likely better represent human population background variation, this variable is best controlled during initial neurobehavioral characterization of NDD-associated genes. Our model also likely suffered from incomplete penetrance of the gene-trap cassette resulting in uncontrolled mosaicism—evident from residual *Kmt5b* expression in KO embryos (~11% of WT; Figure 1A). Other groups have noted a similar issue when targeting *Kmt5b* using a Cre-lox strategy (Neguembor et al., 2013). While use of a CRISPR/Cas9 strategy may have circumvented this problem, we chose to use a KOMP line because it was readily available, had been initially characterized by the International Mouse Phenotyping Consortium (IMPC) (Dickinson et al., 2016), contained a selectable LacZ marker, and could help us to better understand whether mice from this source could be used for systematic phenotyping of the increasing number of NDD risk genes that have been identified over the last decade. We propose that KOMP animals on a C57BL/6N background should be backcrossed to a C56BL/6J strain for the most robust data collection in specifically ASD-associated studies.

Supplementary Material

Refer to Web version on PubMed Central for supplementary material.

Acknowledgments:

We would like to thank the investigators of the Knockout Mouse Project (KOMP) for making available the mouse line used in this study. Particularly, we would like to thank the Mutant Mouse Resource & Research Center (MMRRC) at UC Davis for cryorecovery of this line. This work was funded by the LB692 Nebraska Tobacco Settlement Biomedical Research Development Program, NIGMS GM110768, and the Simons Foundation Autism Research Initiative-Bridge to Independence Award (SFARI 381192) to H.A.F.S.. The authors have no conflicts of interest.

References

Arbuckle EP, Smith GD, Gomez MC, & Lugo JN (2015). Testing for odor discrimination and habituation in mice. J Vis Exp(99), e52615. doi:10.3791/52615 [PubMed: 25992586]

Austin CP, Battey JF, Bradley A, Bucan M, Capecchi M, Collins FS, … Zambrowicz B (2004). The knockout mouse project. Nat Genet, 36(9), 921–924. doi:10.1038/ng0904-921 [PubMed: 15340423]

Bailey KR, & Crawley JN (2009). Methods of Behavior Analysis in Neuroscience (2nd ed.).

Bergmann P, Militzer K, Schmidt P, & Buttner D (1995). Sex differences in age development of a mouse inbred strain: body composition, adipocyte size and organ weights of liver, heart and muscles. Lab Anim, 29(1), 102–109. doi:10.1258/002367795780740447 [PubMed: 7707674]

Boonsanay V, Zhang T, Georgieva A, Kostin S, Qi H, Yuan X, … Braun T (2016). Regulation of Skeletal Muscle Stem Cell Quiescence by Suv4-20h1-Dependent Facultative Heterochromatin Formation. Cell Stem Cell, 18(2), 229–242. doi:10.1016/j.stem.2015.11.002 [PubMed: 26669898]

Brunelli SA, Curley JP, Gudsnuk K, Champagne FA, Myers MM, Hofer MA, & Welch MG (2015). Variations in maternal behavior in rats selected for infant ultrasonic vocalization in isolation. Horm Behav, 75, 78–83. doi:10.1016/j.yhbeh.2015.08.007 [PubMed: 26306860]

Brust V, Schindler PM, & Lewejohann L (2015). Lifetime development of behavioural phenotype in the house mouse (Mus musculus). Front Zool, 12 Suppl 1, S17. doi:10.1186/1742-9994-12-S1-S17 [PubMed: 26816516]

Buitrago MM, Schulz JB, Dichgans J, & Luft AR (2004). Short and long-term motor skill learning in an accelerated rotarod training paradigm. Neurobiol Learn Mem, 81(3), 211–216. doi:10.1016/j.nlm.2004.01.001 [PubMed: 15082022]

Can A, Dao DT, Arad M, Terrillion CE, Piantadosi SC, & Gould TD (2012). The mouse forced swim test. J Vis Exp (59), e3638. doi:10.3791/3638 [PubMed: 22314943]

Chang YC, Cole TB, & Costa LG (2017). Behavioral Phenotyping for Autism Spectrum Disorders in Mice. Curr Protoc Toxicol, 72, 11 22 11–11 22 21. doi:10.1002/cptx.19 [PubMed: 28463420]

Coe BP, Stessman HAF, Sulovari A, Geisheker MR, Bakken TE, Lake AM, … Eichler EE (2019). Neurodevelopmental disease genes implicated by de novo mutation and copy number variation morbidity. Nat Genet, 51(1), 106–116. doi:10.1038/s41588-018-0288-4 [PubMed: 30559488]

Crawley JN (2007). Mouse behavioral assays relevant to the symptoms of autism. Brain Pathol, 17(4), 448–459. doi:10.1111/j.1750-3639.2007.00096.x [PubMed: 17919130]

Curley JP, & Champagne FA (2016). Influence of maternal care on the developing brain: Mechanisms, temporal dynamics and sensitive periods. Front Neuroendocrinol, 40, 52–66. doi:10.1016/j.yfrne.2015.11.001 [PubMed: 26616341]

Curley JP, Davidson S, Bateson P, & Champagne FA (2009). Social enrichment during postnatal development induces transgenerational effects on emotional and reproductive behavior in mice. Front Behav Neurosci, 3, 25. doi:10.3389/neuro.08.025.2009 [PubMed: 19826497]

de Vrij FM, Levenga J, van der Linde HC, Koekkoek SK, De Zeeuw CI, Nelson DL, … Willemsen R (2008). Rescue of behavioral phenotype and neuronal protrusion morphology in Fmr1 KO mice. Neurobiol Dis, 31(1), 127–132. doi:10.1016/j.nbd.2008.04.002 [PubMed: 18571098]

Deacon RM (2013). Measuring motor coordination in mice. J Vis Exp (75), e2609. doi:10.3791/2609 [PubMed: 23748408]

DeFilippis M (2018). Depression in Children and Adolescents with Autism Spectrum Disorder. Children (Basel), 5(9). doi:10.3390/children5090112

Dickinson ME, Flenniken AM, Ji X, Teboul L, Wong MD, White JK, … Murray SA (2016). High-throughput discovery of novel developmental phenotypes. Nature, 537(7621), 508–514. doi:10.1038/nature19356 [PubMed: 27626380]

Dutta S, & Sengupta P (2016). Men and mice: Relating their ages. Life Sci, 152, 244–248. doi:10.1016/j.lfs.2015.10.025 [PubMed: 26596563]

Ellenbroek BA, Derks N, & Park HJ (2005). Early maternal deprivation retards neurodevelopment in Wistar rats. Stress, 8(4), 247–257. doi:10.1080/10253890500404634 [PubMed: 16423713]

Epstein HT (1978). The effect of litter size on weight gain in mice. J Nutr, 108(1), 120–123. doi:10.1093/jn/108.1.120 [PubMed: 619032]

Faundes V, Newman WG, Bernardini L, Canham N, Clayton-Smith J, Dallapiccola B, … Banka S (2017). Histone Lysine Methylases and Demethylases in the Landscape of Human Developmental Disorders. Am J Hum Genet. doi:10.1016/j.ajhg.2017.11.013

Feather-Schussler DN, & Ferguson TS (2016). A Battery of Motor Tests in a Neonatal Mouse Model of Cerebral Palsy. J Vis Exp (117). doi:10.3791/53569

Fombonne E, Roge B, Claverie J, Courty S, & Fremolle J (1999). Microcephaly and macrocephaly in autism. J Autism Dev Disord, 29(2), 113–119. doi:10.1023/a:1023036509476 [PubMed: 10382131]

Franklin K, & Paxinos G (2008). The Mouse Brain in Stereotaxic Coordinates, Compact (3rd ed.).

Gompers AL, Su-Feher L, Ellegood J, Copping NA, Riyadh MA, Stradleigh TW, … Nord AS (2017). Germline Chd8 haploinsufficiency alters brain development in mouse. Nat Neurosci, 20(8), 1062–1073. doi:10.1038/nn.4592 [PubMed: 28671691]

Guy J, Hendrich B, Holmes M, Martin JE, & Bird A (2001). A mouse Mecp2-null mutation causes neurological symptoms that mimic Rett syndrome. Nat Genet, 27(3), 322–326. doi:10.1038/85899 [PubMed: 11242117]

Hansen GM, Markesich DC, Burnett MB, Zhu Q, Dionne KM, Richter LJ, … Abuin A (2008). Large-scale gene trapping in C57BL/6N mouse embryonic stem cells. Genome Res, 18(10), 1670–1679. doi:10.1101/gr.078352.108 [PubMed: 18799693]

Hartley CA, & Lee FS (2015). Sensitive periods in affective development: nonlinear maturation of fear learning. Neuropsychopharmacology, 40(1), 50–60. doi:10.1038/npp.2014.179 [PubMed: 25035083]

Hollocks MJ, Lerh JW, Magiati I, Meiser-Stedman R, & Brugha TS (2019). Anxiety and depression in adults with autism spectrum disorder: a systematic review and meta-analysis. Psychol Med, 49(4), 559–572. doi:10.1017/S0033291718002283 [PubMed: 30178724]

Hurley RW, & Adams MC (2008). Sex, gender, and pain: an overview of a complex field. Anesth Analg, 107(1), 309–317. doi:10.1213/01.ane.0b013e31816ba437 [PubMed: 18635502]

Jorgensen S, Schotta G, & Sorensen CS (2013). Histone H4 lysine 20 methylation: key player in epigenetic regulation of genomic integrity. Nucleic Acids Res, 41(5), 2797–2806. doi:10.1093/nar/gkt012 [PubMed: 23345616]

Kalueff AV, Aldridge JW, LaPorte JL, Murphy DL, & Tuohimaa P (2007). Analyzing grooming microstructure in neurobehavioral experiments. Nat Protoc, 2(10), 2538–2544. doi:10.1038/nprot.2007.367 [PubMed: 17947996]

Kalueff AV, Stewart AM, Song C, Berridge KC, Graybiel AM, & Fentress JC (2016). Neurobiology of rodent self-grooming and its value for translational neuroscience. Nat Rev Neurosci, 17(1), 45–59. doi:10.1038/nrn.2015.8 [PubMed: 26675822]

Kourmouli N, Jeppesen P, Mahadevhaiah S, Burgoyne P, Wu R, Gilbert DM, … Singh PB (2004). Heterochromatin and tri-methylated lysine 20 of histone H4 in animals. J Cell Sci, 117(Pt 12), 2491–2501. doi:10.1242/jcs.01238 [PubMed: 15128874]

Landers MS, & Sullivan RM (2012). The development and neurobiology of infant attachment and fear. Dev Neurosci, 34(2–3), 101–114. doi:10.1159/000336732 [PubMed: 22571921]

Loomes R, Hull L, & Mandy WPL (2017). What Is the Male-to-Female Ratio in Autism Spectrum Disorder? A Systematic Review and Meta-Analysis. J Am Acad Child Adolesc Psychiatry, 56(6), 466–474. doi:10.1016/j.jaac.2017.03.013 [PubMed: 28545751]

Luong TN, Carlisle HJ, Southwell A, & Patterson PH (2011). Assessment of motor balance and coordination in mice using the balance beam. J Vis Exp (49). doi:10.3791/2376

Machado L, & Relaix F (2016). Heterochromatin compaction is regulated by Suv4-20h1 to maintains skeletal muscle stem cells quiescence. Stem Cell Investig, 3, 23. doi:10.21037/sci.2016.06.04

Madsen GF, Bilenberg N, Cantio C, & Oranje B (2014). Increased prepulse inhibition and sensitization of the startle reflex in autistic children. Autism Res, 7(1), 94–103. doi:10.1002/aur.1337 [PubMed: 24124111]

Matsuo N, Takao K, Nakanishi K, Yamasaki N, Tanda K, & Miyakawa T (2010). Behavioral profiles of three C57BL/6 substrains. Front Behav Neurosci, 4, 29. doi:10.3389/fnbeh.2010.00029 [PubMed: 20676234]

Mena A, Ruiz-Salas JC, Puentes A, Dorado I, Ruiz-Veguilla M, & De la Casa LG (2016). Reduced Prepulse Inhibition as a Biomarker of Schizophrenia. Front Behav Neurosci, 10, 202. doi:10.3389/fnbeh.2016.00202 [PubMed: 27803654]

Mizoguchi T, Minakuchi H, Ishisaka M, Tsuruma K, Shimazawa M, & Hara H (2017). Behavioral abnormalities with disruption of brain structure in mice overexpressing VGF. Sci Rep, 7(1), 4691. doi:10.1038/s41598-017-04132-7 [PubMed: 28680036]

Myers KM, & Davis M (2007). Mechanisms of fear extinction. Mol Psychiatry, 12(2), 120–150. doi:10.1038/sj.mp.4001939 [PubMed: 17160066]

Neguembor MV, Xynos A, Onorati MC, Caccia R, Bortolanza S, Godio C, … Gabellini D (2013). FSHD muscular dystrophy region gene 1 binds Suv4-20h1 histone methyltransferase and impairs myogenesis. J Mol Cell Biol, 5(5), 294–307. doi:10.1093/jmcb/mjt018 [PubMed: 23720823]

Oda H, Okamoto I, Murphy N, Chu J, Price SM, Shen MM, … Reinberg D (2009). Monomethylation of histone H4-lysine 20 is involved in chromosome structure and stability and is essential for mouse development. Mol Cell Biol, 29(8), 2278–2295. doi:10.1128/MCB.01768-08 [PubMed: 19223465]

Paquin KL, & Howlett NG (2018). Understanding the Histone DNA Repair Code: H4K20me2 Makes Its Mark. Mol Cancer Res, 16(9), 1335–1345. doi:10.1158/1541-7786.MCR-17-0688 [PubMed: 29858375]

Pellegrino S, Michelena J, Teloni F, Imhof R, & Altmeyer M (2017). Replication-Coupled Dilution of H4K20me2 Guides 53BP1 to Pre-replicative Chromatin. Cell Rep, 19(9), 1819–1831. doi:10.1016/j.celrep.2017.05.016 [PubMed: 28564601]

Philip VM, Duvvuru S, Gomero B, Ansah TA, Blaha CD, Cook MN, … Chesler EJ (2010). High-throughput behavioral phenotyping in the expanded panel of BXD recombinant inbred strains. Genes Brain Behav, 9(2), 129–159. doi:10.1111/j.1601-183X.2009.00540.x [PubMed: 19958391]

Pitts MW (2018). Barnes Maze Procedure for Spatial Learning and Memory in Mice. Bio Protoc, 8(5). doi:10.21769/bioprotoc.2744

Reed DR, Bachmanov AA, & Tordoff MG (2007). Forty mouse strain survey of body composition. Physiol Behav, 91(5), 593–600. doi:10.1016/j.physbeh.2007.03.026 [PubMed: 17493645]

Rosenfeld CS, & Ferguson SA (2014). Barnes maze testing strategies with small and large rodent models. J Vis Exp (84), e51194. doi:10.3791/51194 [PubMed: 24637673]

Satterstrom FK, Kosmicki JA, Wang J, Breen MS, De Rubeis S, An JY, … Buxbaum JD (2020). Large-Scale Exome Sequencing Study Implicates Both Developmental and Functional Changes in the Neurobiology of Autism. Cell, 180(3), 568–584 e523. doi:10.1016/j.cell.2019.12.036 [PubMed: 31981491]

Schiller D, & Delgado MR (2010). Overlapping neural systems mediating extinction, reversal and regulation of fear. Trends Cogn Sci, 14(6), 268–276. doi:10.1016/j.tics.2010.04.002 [PubMed: 20493762]

Schotta G, Lachner M, Sarma K, Ebert A, Sengupta R, Reuter G, … Jenuwein T (2004). A silencing pathway to induce H3-K9 and H4-K20 trimethylation at constitutive heterochromatin. Genes Dev, 18(11), 1251–1262. doi:10.1101/gad.300704 [PubMed: 15145825]

Schotta G, Sengupta R, Kubicek S, Malin S, Kauer M, Callen E, … Jenuwein T (2008). A chromatin-wide transition to H4K20 monomethylation impairs genome integrity and programmed DNA rearrangements in the mouse. Genes Dev, 22(15), 2048–2061. doi:10.1101/gad.476008 [PubMed: 18676810]

Seibenhener ML, & Wooten MC (2015). Use of the Open Field Maze to measure locomotor and anxiety-like behavior in mice. J Vis Exp (96), e52434. doi:10.3791/52434 [PubMed: 25742564]

Shoji H, Takao K, Hattori S, & Miyakawa T (2016). Age-related changes in behavior in C57BL/6J mice from young adulthood to middle age. Mol Brain, 9, 11. doi:10.1186/s13041-016-0191-9 [PubMed: 26822304]

Silverman JL, Yang M, Lord C, & Crawley JN (2010). Behavioural phenotyping assays for mouse models of autism. Nat Rev Neurosci, 11(7), 490–502. doi:10.1038/nrn2851 [PubMed: 20559336]

Simonetta M, de Krijger I, Serrat J, Moatti N, Fortunato D, Hoekman L, … Jacobs JJL (2018). H4K20me2 distinguishes pre-replicative from post-replicative chromatin to appropriately direct DNA repair pathway choice by 53BP1-RIF1-MAD2L2. Cell Cycle, 17(1), 124–136. doi:10.1080/15384101.2017.1404210 [PubMed: 29160738]

Singewald N, & Holmes A (2019). Rodent models of impaired fear extinction. Psychopharmacology (Berl), 236(1), 21–32. doi:10.1007/s00213-018-5054-x [PubMed: 30377749]

Stessman HA, Xiong B, Coe BP, Wang T, Hoekzema K, Fenckova M, … Eichler EE (2017). Targeted sequencing identifies 91 neurodevelopmental-disorder risk genes with autism and developmental-disability biases. Nat Genet, 49(4), 515–526. doi:10.1038/ng.3792 [PubMed: 28191889]

Takao K, & Miyakawa T (2006). Light/dark transition test for mice. J Vis Exp(1), 104. doi:10.3791/104 [PubMed: 18704188]

Trinh J, Kandaswamy KK, Werber M, Weiss MER, Oprea G, Kishore S, … Rolfs A (2019). Novel pathogenic variants and multiple molecular diagnoses in neurodevelopmental disorders. J Neurodev Disord, 11(1), 11. doi:10.1186/s11689-019-9270-4 [PubMed: 31238879]

Tucker LB, Fu AH, & McCabe JT (2016). Performance of Male and Female C57BL/6J Mice on Motor and Cognitive Tasks Commonly Used in Pre-Clinical Traumatic Brain Injury Research. J Neurotrauma, 33(9), 880–894. doi:10.1089/neu.2015.3977 [PubMed: 25951234]

Vougiouklakis T, Sone K, Saloura V, Cho HS, Suzuki T, Dohmae N, … Hamamoto R (2015). SUV420H1 enhances the phosphorylation and transcription of ERK1 in cancer cells. Oncotarget, 6(41), 43162–43171. doi:10.18632/oncotarget.6351 [PubMed: 26586479]

Walf AA, & Frye CA (2007). The use of the elevated plus maze as an assay of anxiety-related behavior in rodents. Nat Protoc, 2(2), 322–328. doi:10.1038/nprot.2007.44 [PubMed: 17406592]

Wickramasekara RN, & Stessman HAF (2019). Histone 4 Lysine 20 Methylation: A Case for Neurodevelopmental Disease. Biology (Basel), 8(1). doi:10.3390/biology8010011

Wu Y, Wang Y, Liu M, Nie M, Wang Y, Deng Y, … Zhao Q (2018). Suv4-20h1 promotes G1 to S phase transition by downregulating p21(WAF1/CIP1) expression in chronic myeloid leukemia K562 cells. Oncol Lett, 15(5), 6123–6130. doi:10.3892/ol.2018.8092 [PubMed: 29616094]

Yadav R, Hillman BG, Gupta SC, Suryavanshi P, Bhatt JM, Pavuluri R, … Dravid SM (2013). Deletion of glutamate delta-1 receptor in mouse leads to enhanced working memory and deficit in fear conditioning. PLoS One, 8(4), e60785. doi:10.1371/journal.pone.0060785 [PubMed: 23560106]

Yang M, & Crawley JN (2009). Simple behavioral assessment of mouse olfaction. Curr Protoc Neurosci, *Chapter* 8, Unit 8 24. doi:10.1002/0471142301.ns0824s48 [PubMed: 19575474]

Yang M, Silverman JL, & Crawley JN (2011). Automated three-chambered social approach task for mice. Curr Protoc Neurosci, *Chapter* 8, Unit 8 26. doi:10.1002/0471142301.ns0826s56 [PubMed: 21732314]

Zhou J, Blundell J, Ogawa S, Kwon CH, Zhang W, Sinton C, … Parada LF (2009). Pharmacological inhibition of mTORC1 suppresses anatomical, cellular, and behavioral abnormalities in neural-specific Pten knock-out mice. J Neurosci, 29(6), 1773–1783. doi:10.1523/JNEUROSCI.5685-08.2009 [PubMed: 19211884]

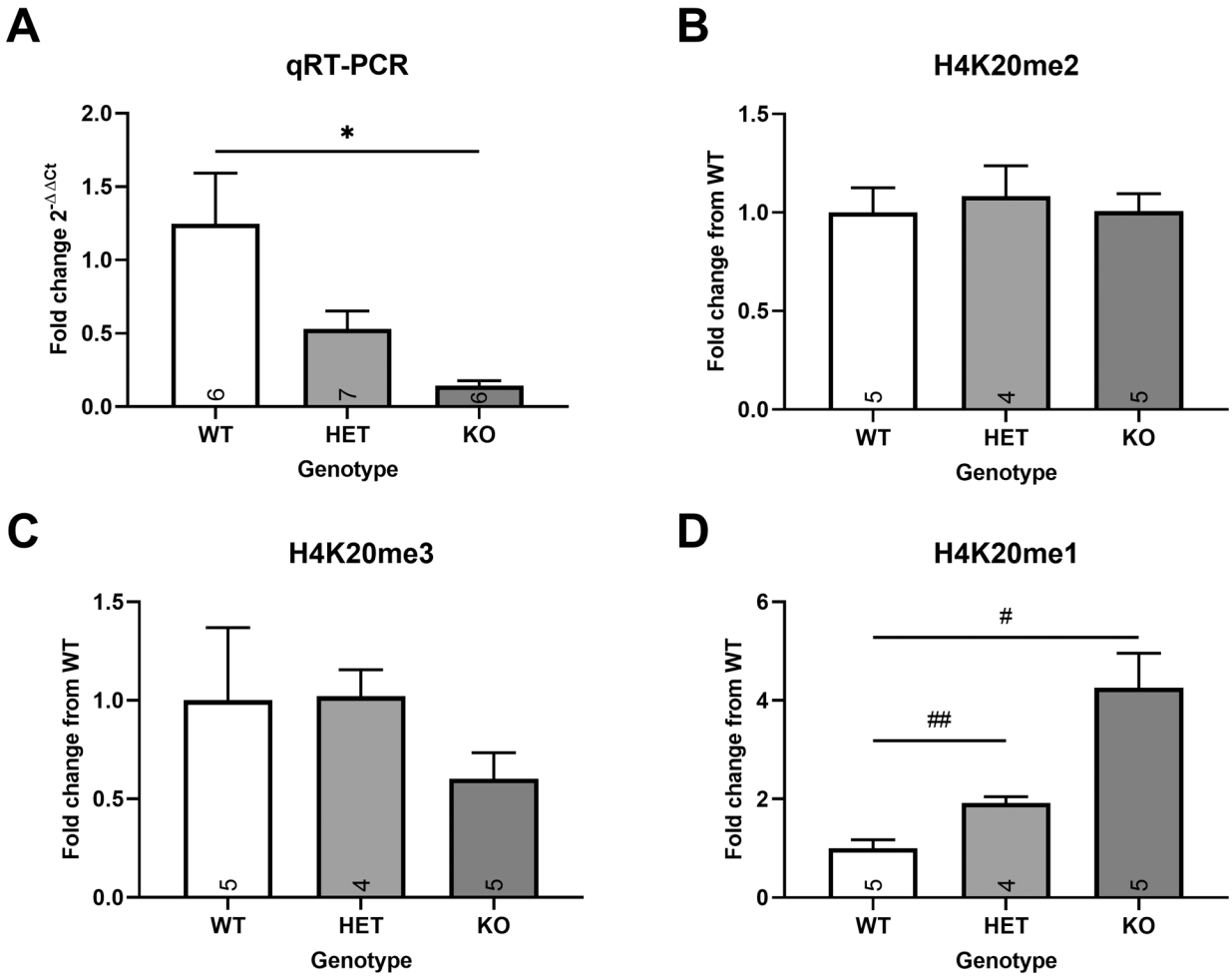

Figure 1.

Kmt5b expression and H4K20 methylation levels in the *Kmt5b* gene-trap mouse model. (**A**) qRT-PCR validation of *Kmt5b* knock-out efficiency (exon 7–8 junction), KO N=6. (**B**) H4K20me2, (**C**) H4K20me3, and (**D**) H4K20me1 protein levels detected by western blot in E14.5 embryonic brain tissue from HET x HET progeny. *significant by ANOVA; #significant by post-hoc test. Data show the mean ± SEM.

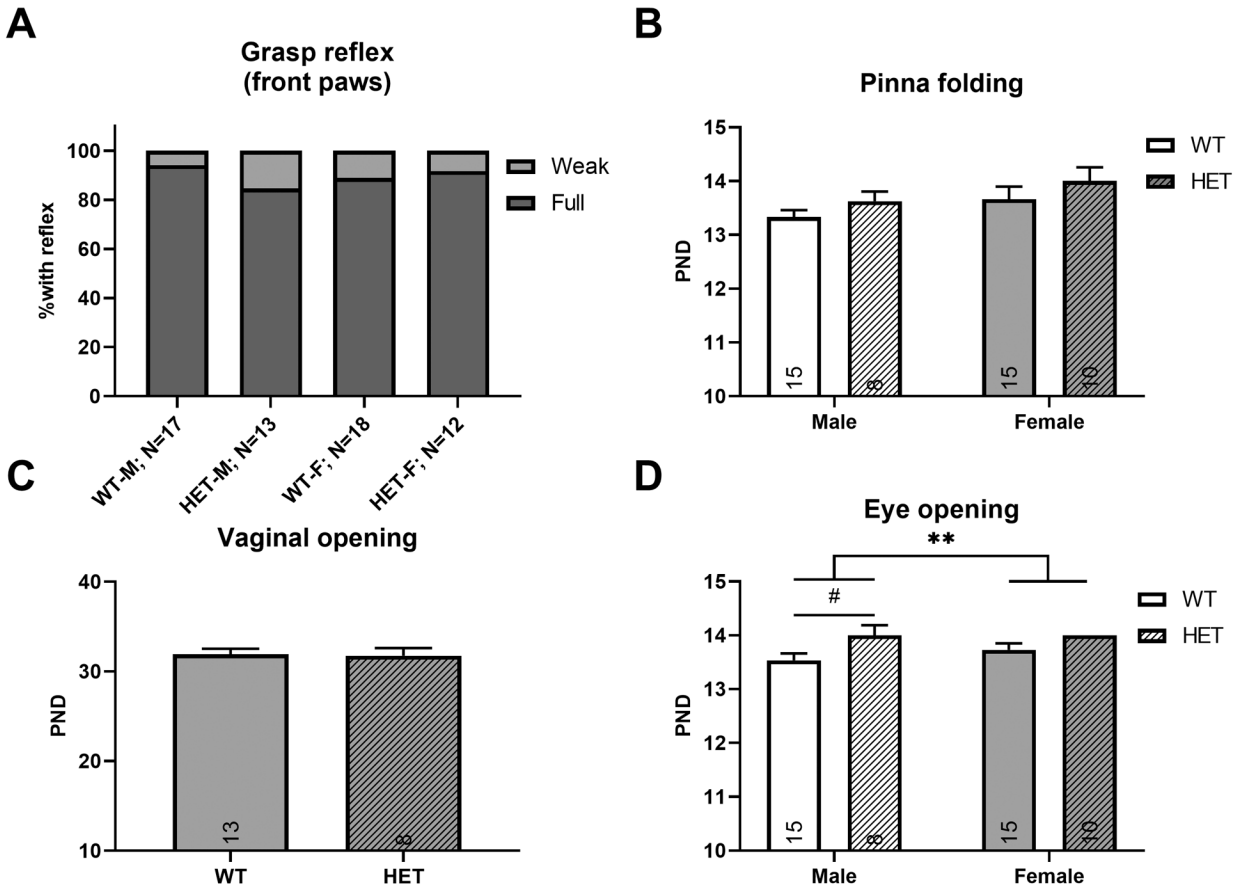

Figure 2.

Milestone markers in *Kmt5b* mice. (**A**) Presence of the palmar grasp reflex in front paws is shown on PND10 for each group. Dark gray=full response; light gray=weak response. Ages of (**B**) pinna folding, (**C**) vaginal opening (females only), and (**D**) eye opening are shown between genotypes and sexes. For B-D, solid white bars=WT male, hatched white bars=HET male; solid gray bars=WT female; hatched gray bars=HET female; *significant by ANOVA; #significant by post-hoc test. Data show the mean ± SEM.

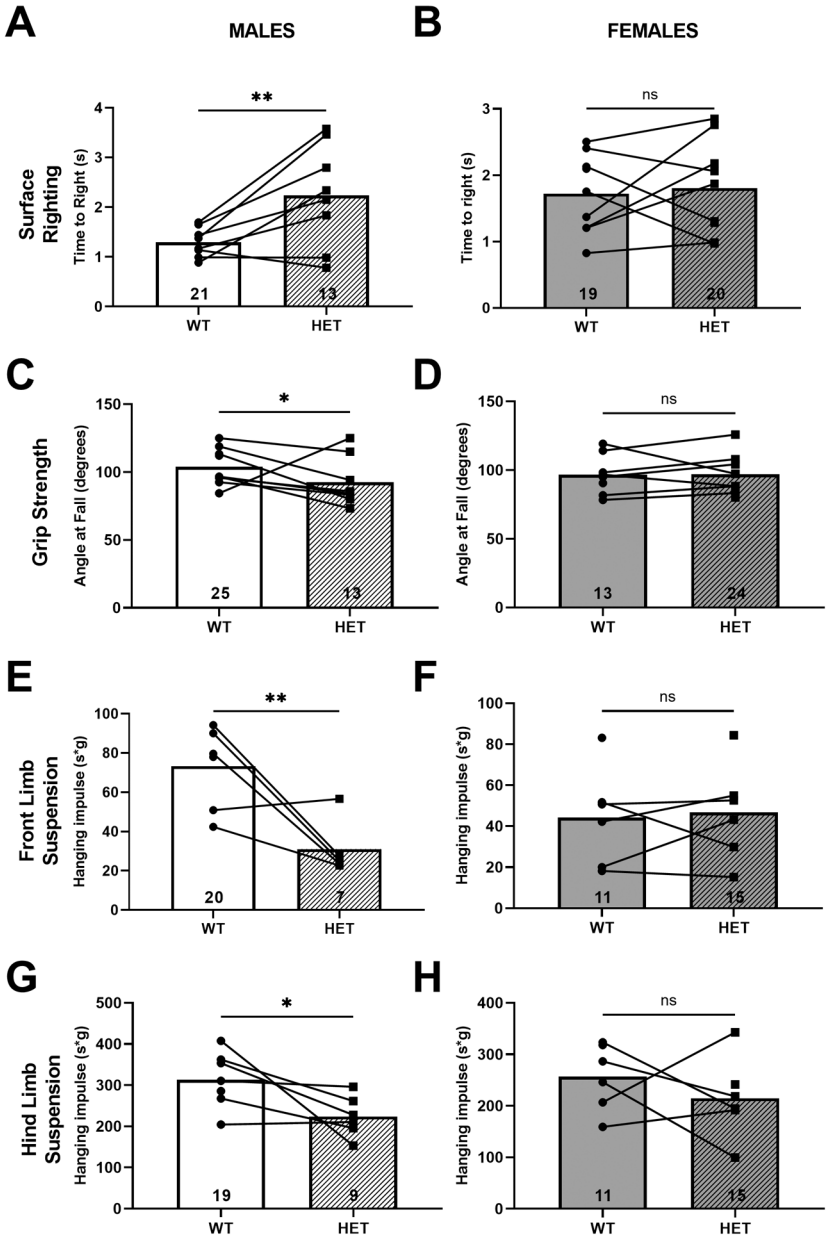

Figure 3.

Neonatal tests. All data are plotted as averages by litter (connecting lines). (**A-B**) Surface righting test shown as time to right (s) and (**C-D**) grip strength test shown as the angle at fall (degrees). (**E-F**) Front limb and (**G-H**) hind limb suspension tests shown as the hanging impulse (suspension time (s) x weight (g)). Solid white bars=WT male, hatched white bars=HET male; solid gray bars=WT female; hatched gray bars=HET female; connecting lines between points show WT vs HET mice from the same litter. *significant by 2-way ANOVA (litter x genotype); sexes were analyzed separately.

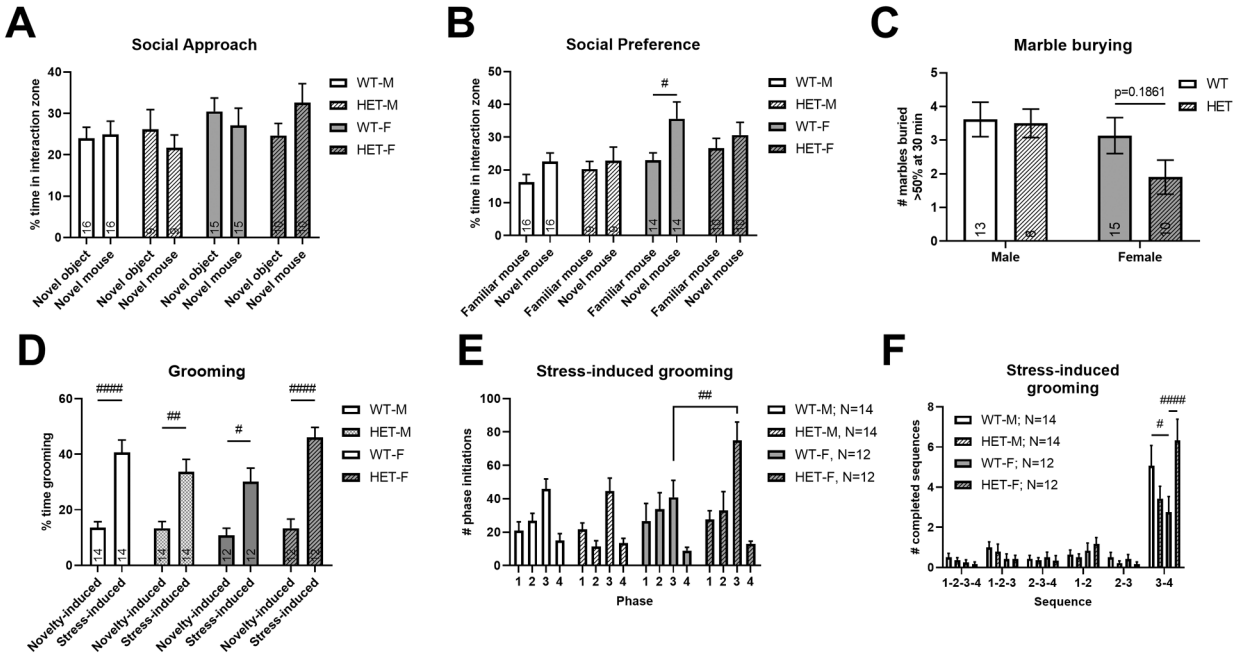

Figure 4.

Social and repetitive behaviors tests. (**A**) All mice show a lack of sociability in the social approach test. (**B**) Only female WT mice show sociability in the social preference test. (**C**) No differences were seen in the number of marbles buried in the marble burying test. (**D**) Total time spent grooming is increased after stress (misted with water) for all mice. (**E**) Stress-induced grooming increased bilateral stroke initiations (head grooming) in HET females only due to an (**F**) increased phase 3–4 cephalo-caudal grooming sequence. Solid white bars=WT male, hatched white bars=HET male; solid gray bars=WT female; hatched gray bars=HET female; *significant by ANOVA; #significant by post-hoc test. p-values shown are from post hoc testing. Data show the mean ± SEM.

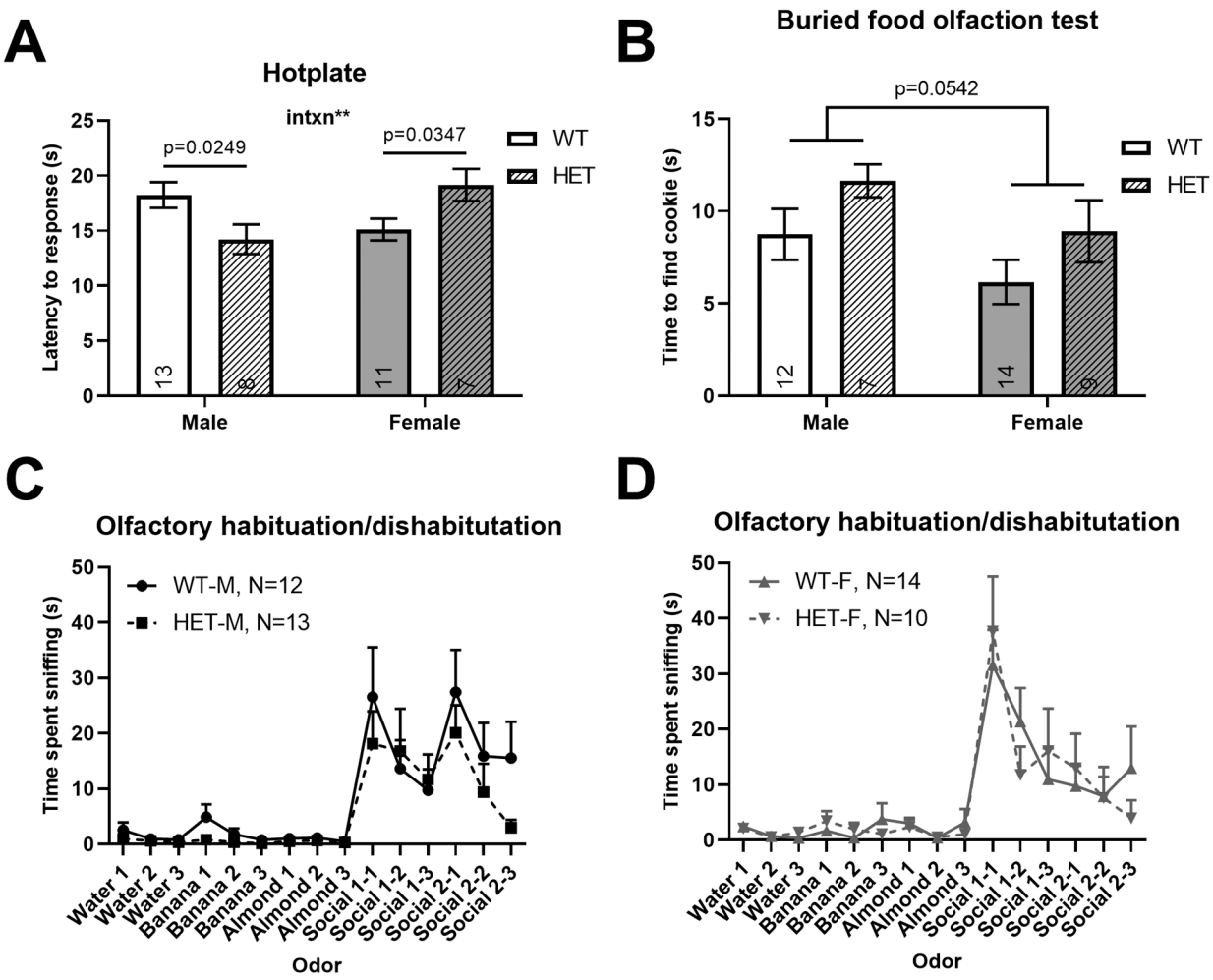

Figure 5.

Sensory tests. (**A**) In the hot plate test, male HET mice showed decreased tolerance to heat while female HET mice showed increased tolerance, suggesting sexual dimorphism. p-values shown for this test are from post hoc testing. p-values shown are from post hoc testing. (**B**) No significant differences were seen in the time to retrieve a buried food pellet for male or female HET mice. (**C-D**) The time spent sniffing both non-social and social odors were similar for male and female, WT and HET mice. Solid white bars/black lines=WT male, hatched white bars/black lines=HET male; solid gray bars/lines=WT female; hatched gray bars/lines=HET female; *significant by ANOVA. p-values shown are from post hoc testing. Data show the mean ± SEM.

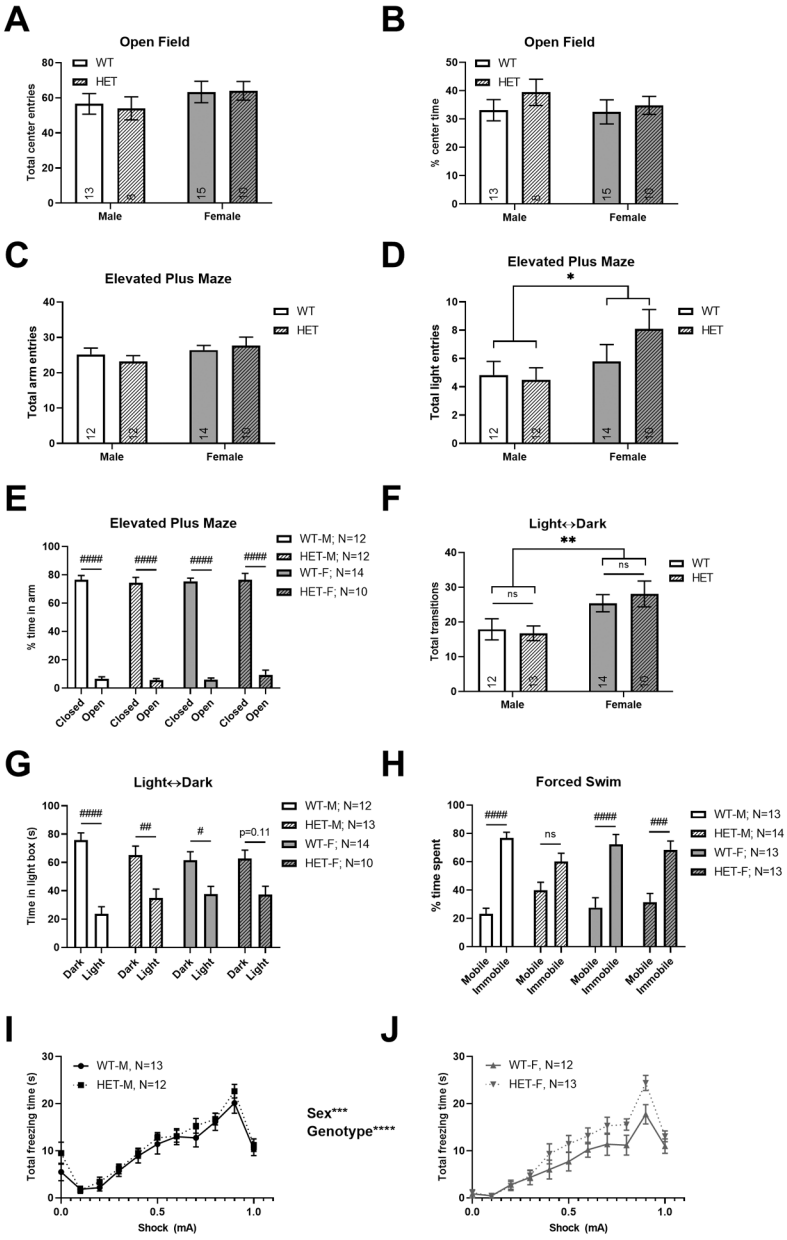

Figure 6.

Novel exploration, anxiety, depression, and fear tests. Compared to WT mice, HET mice did not show any differences in (**A**) total center entries or (**B**) percent time spent in the center of the open field test. No genotype differences were seen in the (**C**) total arm entries, (**D**) total light arm entries, or the (**E**) percent time spent in the closed vs open arms of the elevated plus-maze. (**F**) Female mice had an increased number of transitions between light and dark compartments in the light↔dark transition test; however, no genotype differences were observed. (**G**) HET mice, overall, showed less preference for the dark compartment independent of sex. (**H**) Female WT and HET mice performed similarly in the forced swim test. However, WT male mice spent a relatively larger amount of time immobile in this test compared to HET males. (**I-J**) Increasing intensity of foot shocks were associated with

increased fear (measured as freezing) in HET animals. Solid white bars/lines=WT male, hatched white bars/black lines=HET male; solid gray bars/black lines=WT female; hatched gray bars/lines=HET female; *significant by ANOVA; #significant by post-hoc test; ns=not significant. p-values shown are from post hoc testing. Data show the mean ± SEM.

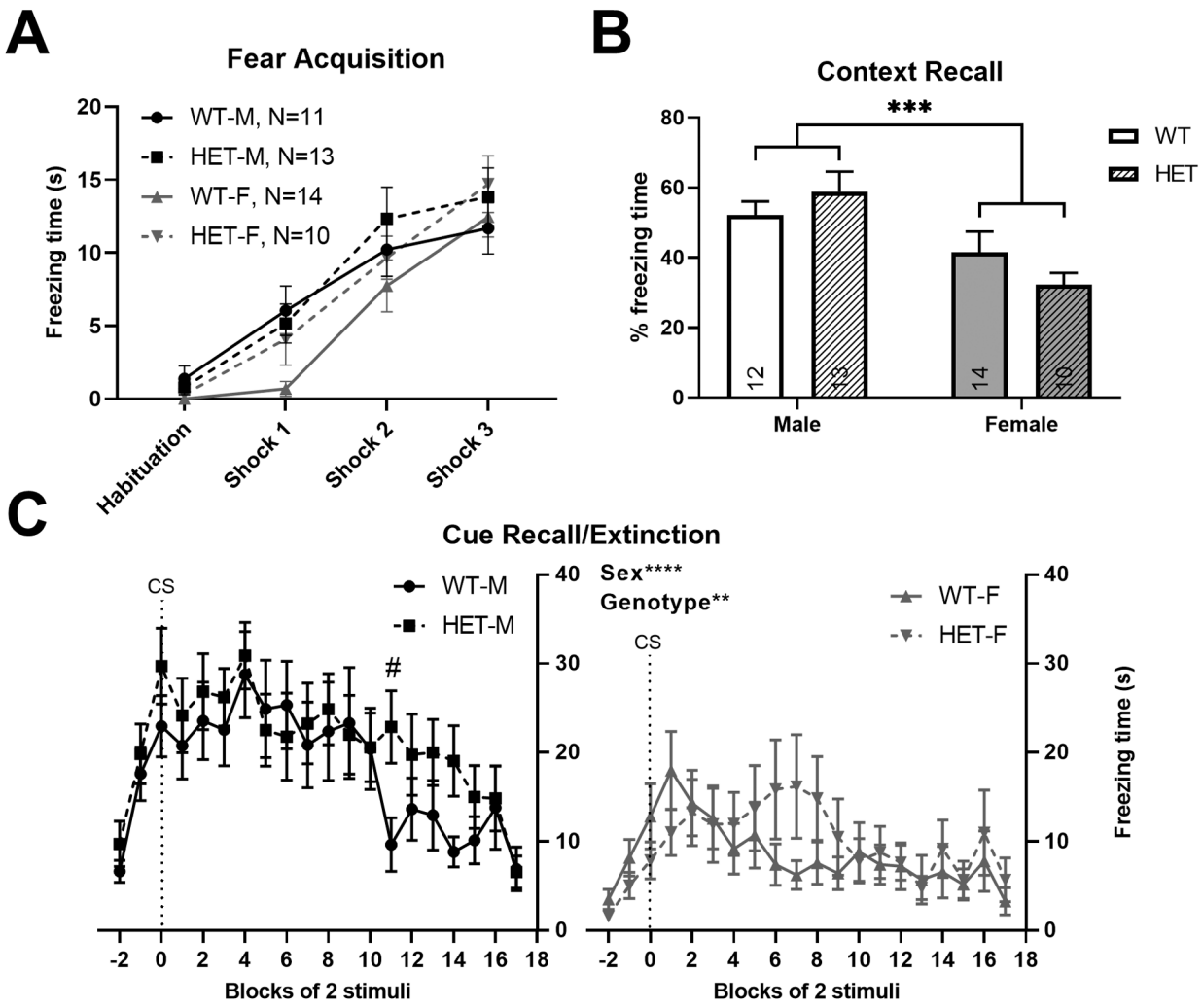

Figure 7.

Fear learning, acquisition, and recall tests. (**A**) All mice acquire fear to a similar degree in the first day. Time spent freezing for 30 s following each US-CS presentation is plotted on the y-axis. (**B**) Females show significantly lower context recall than males. HET animals show sexually dimorphic effects during recall. (**C**) Changing the context and adding back the conditioned stimulus (CS) showed that animals have fear renewal (change before and after CS), but extinction is delayed in HET compared to WT animals. X-axis shows blocks of 2 stimuli (60 s each) following presentation of the CS (WT-M=12; WT-F=14; HET-M=13; HET-F=10). Solid white bars/black lines=WT male, hatched white bars/black lines=HET male; solid gray bars/lines=WT female; hatched gray bars/lines=HET female; *significant by ANOVA; #significant by post-hoc test; data show the mean ± SEM.

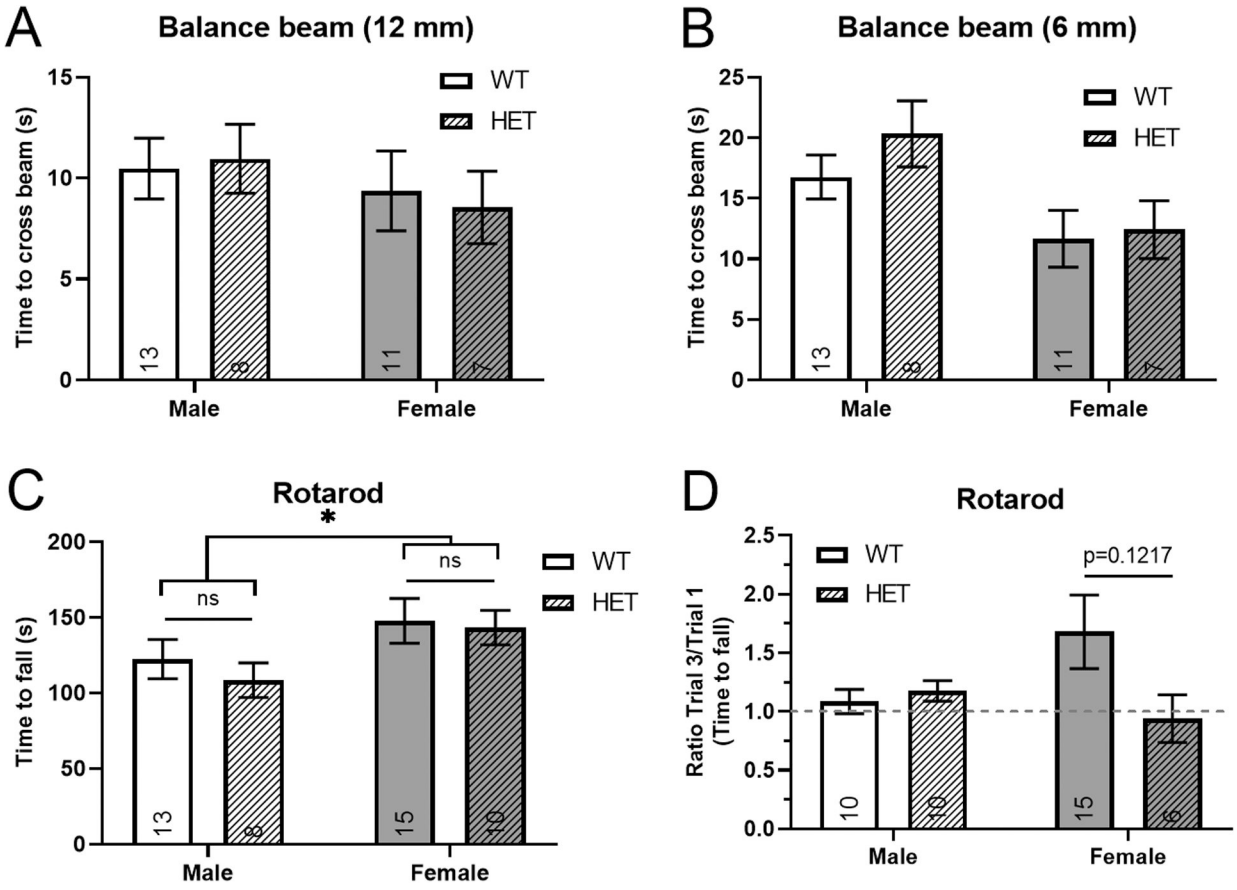

Figure 8.

Adult motor tests. No differences were seen in the time taken to cross a (**A**) 12 mm or (**B**) 6 mm elevated balance beam. In the rotarod test, (**C**) females stayed on the rotarod longer than males; however, there was no difference between WT and HET mice. (**D**) Time to fall trial 3/trial 1 on the rotarod did not show significant learning differences between sexes or genotypes. Solid white bars=WT male, hatched white bars=HET male; solid gray bars=WT female; hatched gray bars=HET female; *significant by ANOVA; ns=not significant. p-value shown is from post hoc testing. Data show the mean ± SEM.

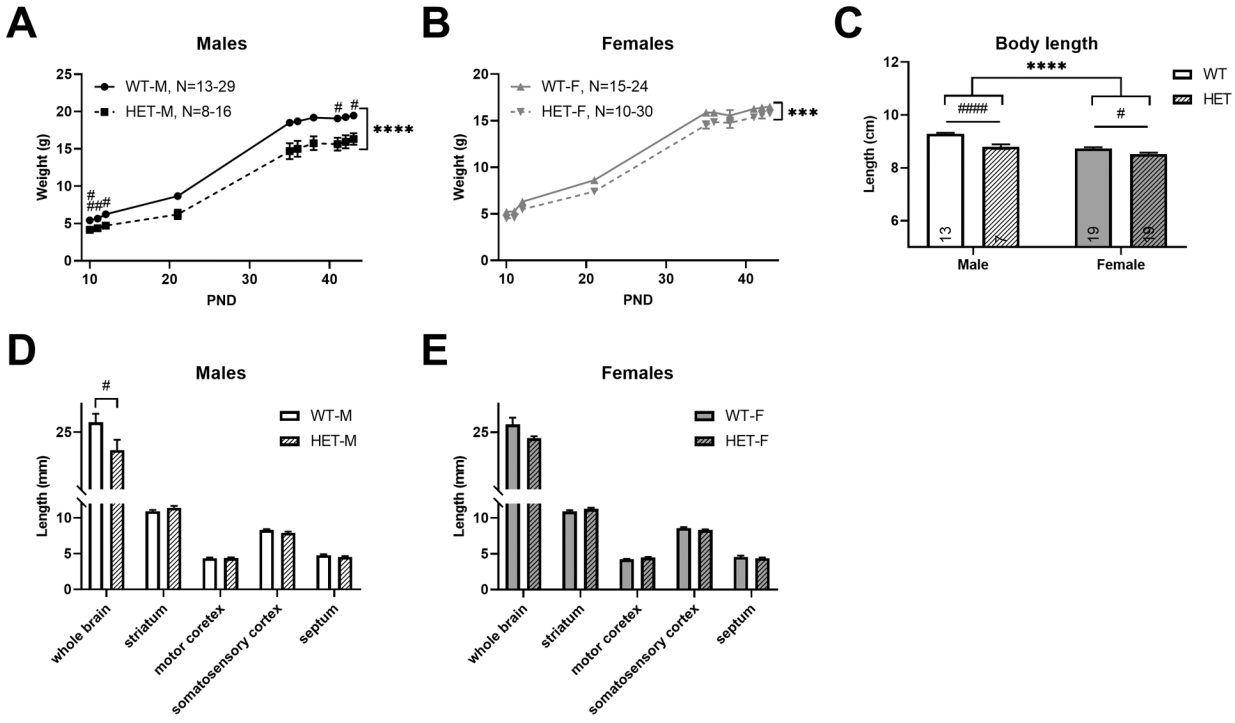

Figure 9.

Body weight, length, and brain size differences. Weight measurements taken over the testing period (postnatal days 10–44) show that HET animals are lighter than WTs; this is more severe in males (**A**) than females (**B**). (**C**) HETs also have significantly shorter body lengths than WT mice, which is more significant in males. (**D**) Male HET mice show reduced whole brain size compared to WT mice (N=7 per genotype), while (**E**) female mice (N=6 per genotype) do not show a significant difference. Solid white bars/black lines=WT male, hatched white bars/black lines=HET male; solid gray bars/lines=WT female; hatched gray bars/lines=HET female; *significant by ANOVA; #significant by post-hoc test. Data show the mean ± SEM.

Table 1.

Genotype frequencies in offspring.

	Total # of animals	Observed # of pups			Expected # of pups				
Timepoint		**WT**	**HET**	**KO**	**WT**	**HET**	**KO**	**Chi-square value, df**	**P value**
E14.5	99	17	63	19	25	50	25	3.833, 2	0.1471
E16.5-E18.5	21	1	12	8	5	10	5	3.518, 2	0.1722
P0	41	11	28	2	10	20	10	6.703, 2	**0.035**
Adult	44	16	28	0	11	22	11	9.969, 2	**0.0068**

Df: degrees of freedom